Application of Fluorometers to Measure Wild Algal Growth *In Vivo*

Raymond Delashmitt

Abstract

The goal of this project was to characterize the WetLabs FLNTUSB fluorometer and determine the possibility of using it as an instrument to measure wild algal growth on substrates in vivo. To do this several aspects were investigated, which include determining the angle sensitivity of the instruments, if the instruments were able to compared directly to each other, if the signals recorded demonstrated that the instruments were recording actual fluorescence of algae, and to correlate the signal recorded to harvest data during the same time period. The results of this investigation showed that the angle sensitivity depends on whether the angle from normal is within the beam plane created by the LED and absorption cones, or if it was perpendicular to the beam plane. In the investigation to determine if the fluorometers were observing actual fluorescence of chlorophyll in the algae, it was determined that the signal was from fluorescence due to a photo-inhibition effect and the variance being dependent on the size of the signal. Finally, there is evidence that the fluorescence observed during the deployments of this project can be compared to harvest data during the same time period and the relative changes in both of these data sets appear to match, especially during periods that the substrates the fluorometers were observing were cleaned and the signal dropped accordingly.

Fluorometer Background

Fluorometers have been widely used since the early 1970's in marine biology research applications and it has been proven they can accurately model the level of chlorophyll in the

water. It has also been shown previously that by detecting the chlorophyll, the fluorometer can measure a sample's level of ambient algae in water.[1] This technique of measuring algae growth has become a popular and widely accepted process due to the fact that the measurement can be done accurately, in real-time, without needing to remove the algae from the environment, and with a handheld instrument. Previous solutions to measuring algae involved removing the algae from the water by taking water samples, then measuring the algae populations in a lab with counting chamber methods[2] or High Performance Liquid Chromatography[3].

The fluorometer measures the level of chlorophyll by the amount that the object in the beam fluoresces. The meter sends out a LED light of wavelength 470 nm, and when it comes in contact with the *chlorophyll a* in the algae it is absorbed, exciting it to a higher quantum state that then emits a photon back out at a wavelength of 695 nm[4]. This process is shown in **figure 1**[5] below, with the LED as the transmitter, and the algae represented as the *chlorophyll a* molecules.

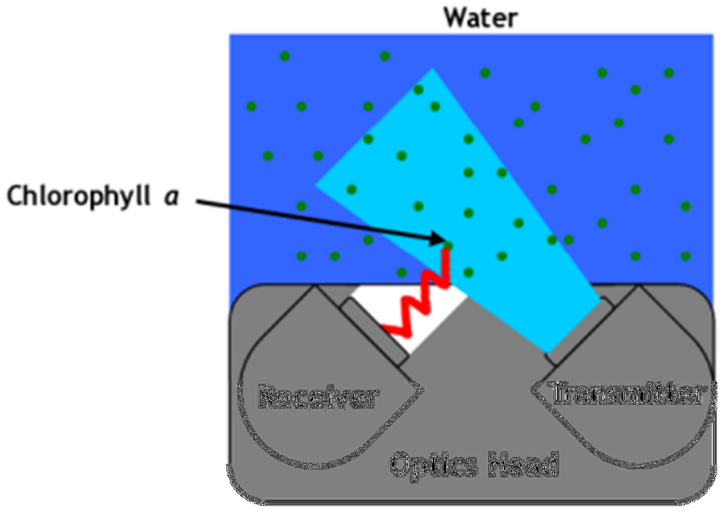

Figure 1
Diagram showing absorption of the LED photon and reemission of a photon to the detector

[1](Aberle, September 2006)
[2](H Utermoehl, 1958)
[3](Schroeder, 1994)
[4](Wetlabs, 23 Dec 2009)
[5](SCCF Recon, 2010)

The data from the fluorometer is recorded as a digital count or an analog voltage. The digital counts range from 50 to 4130, and the analog ranges from .072 V to 4.98 V. This means that the fluorometers feature a dark count of 50, which is present in all data collected, and in all the graphs featured, will have this value subtracted to give only the signals received by the fluorometers.

Additionally, due to the nature of the fluorescence of the chlorophyll, an issue with the detection is that the photon emitted from the algae is emitted in a random direction. Thus, the meter is set up to do an average of a set number of samples to decrease the noise in the signal. In these samples a variance is expected, which should be related to the signal strength by a square root function. For all of the samples taken during the experiments, the average number of data values taken before generating a single point was 60, then in the analysis of the data for hourly and daily averages each of these single points were used.

Lab Experiments

For the controlled lab tests to measure the configuration of the fluorometers, the experiments were to measure the angle of the local maxima of the signal produced by the instruments when exposed to a point-like source of fluorescence and to measure the angles of dispersion of the LED source and the cone of detection. To measure the angles of dispersion of the LED, a reflective surface was used to allow tracing of the light cone, which resulted in the following measurements in **figure 2**. This recorded line was of the sharp edge the beam dispersed by the LED, with the intensity dropping off substantially outside of the 15 degrees recorded. This area of light shall be referred to as the maximum LED cone.

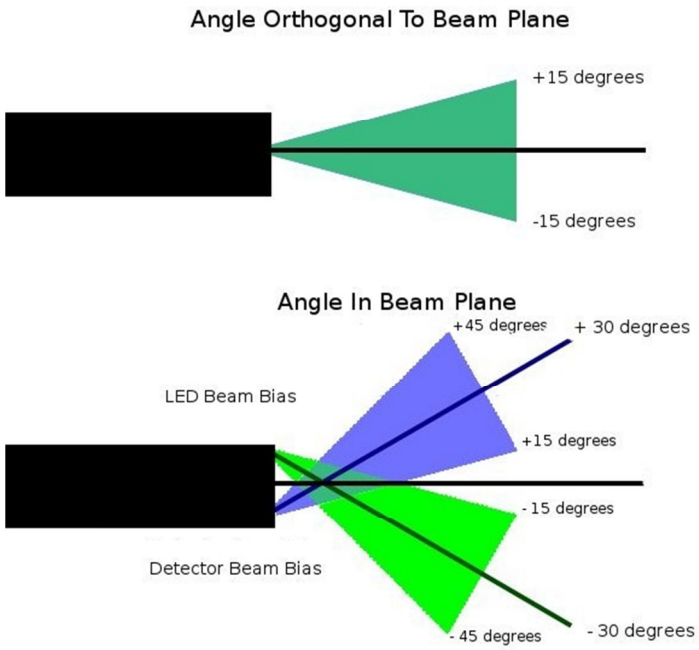

Figure 2
Diagram of the LED and absorption cones

The colored portions of the diagram show the areas that are the maximum LED dispersion or detector absorption cones. The maximum light dispersion cone was measured, while the cone of maximum absorption was based off of orientation of the detector with the assumption of it behaving in reverse to the LED photon dispersion beam. The absorption cone was drawn based on the symmetry to the light cone and geometry of the detector offset from normal. These cones are not the only areas that signal is detected by the fluorometer due to the Gaussian decay of the signal. This decay of the signal allows the tails of the two cones to intersect in front of the face of the instrument, which accounts for signal recorded by the fluorometer in the angle study experiment. In the diagram, it shows how when the angle is not in the plane where the beams cross, the theoretical dispersion is the same, and should result in the least amount of distortion of the signal. When the angle is measured in the beam plane, the geometry shows the cones of the LED and detector with an offset of 15 degrees towards each other, and each of the cones having a 15 degrees spread. This dispersion results in a theoretical range between .5 cm and 1.8 cm

where the signal is maximum, which is shown in later experiments to result in an oversaturated signal.

The next experiments were to determine the sensitivity of the fluorometers to a change in angle when the distance was held constant. The first experiment was to use a point-like source of 1 cm radius as the source of the fluorescence and to go through the entire range of angles possible to the fluorometers. The experiment had the change of angle both orthogonal to and within the plane that the LED and detector cone beams intersect. In this setup, the data was taken at intervals of 10 degrees while the radial distance of the face of the fluorometer to the substrate was held constant. The range of angles represented express the range of freedom that the biowiper and the size of the fluorometers allow, generally 70 degrees from normal in either direction.

The data for when the angle was perpendicular to the plane resulted with the absolute maximum at 90 degrees to the substrate with the signal decaying as the angle deviated from this value. On the closer distances the physical offset of the LED and detector, in the design of the instrument to account for the biowiper, affected my ability to keep the same distance on either side from normal. This resulted in the curve being biased towards the angles where the open biowiper is farthest away from the substrate due to its relative closer proximity to the substrate. The data from this experiment is featured in **figure 3** below with the dark counts accounted for in the signal.

The next aspect was when the angle was in the beam plane where the data showed signs from the previous analysis of the local maxima of the signal, but with the maximum directly in front of the LED beam being much larger than the other maxima present in the signal. The secondary maximum that was observed in some of the signals was towards the theoretical beam

that is directly in front of the detector, and is greatest when the distances to the substrate are smallest. The maximum of the signal shifted as the distances away from the substrate changed. This shows evidence of an interaction between the LED and detectors cones that pulling of the maxima towards normal is occurring, due to the decay tails limiting the amount of photons available to be detected along the previously stated angles. At the smallest distance of 3 cm away, the maximum was at 20 degrees from normal towards the LED beam side. At the larger distances of 5, 7, and 8 cm away, the maximum was between 40 and 50 degrees from normal, towards the LED beam side. The other signals are between the 20 – 50 degrees from normal towards the LED beam side. This data of this experiment is featured in below in **figure 4** and features the complete dataset with 6 points taken for each angle to show the spread of data for certain angles and a subtraction of the dark counts.

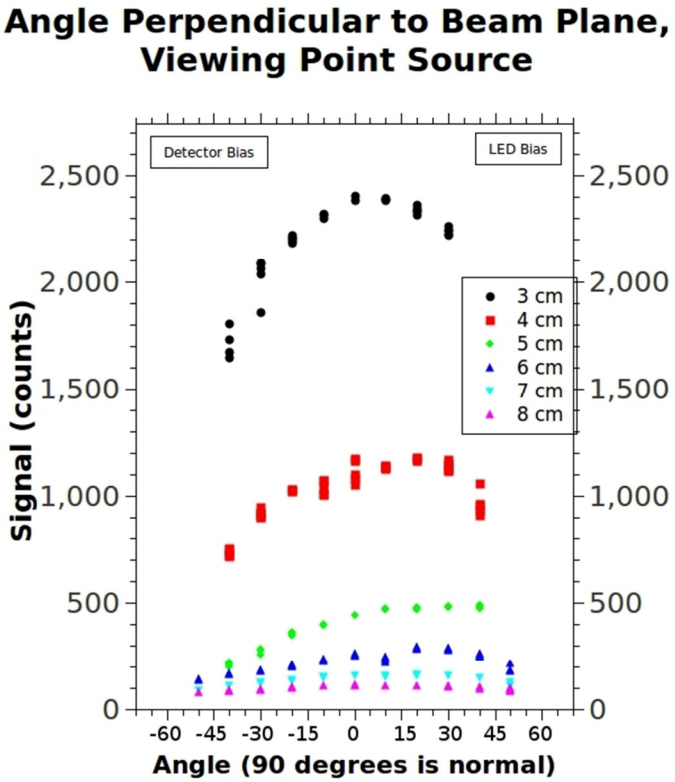

Figure 3
Angle study with angle perpendicular to beam plane and viewing point source

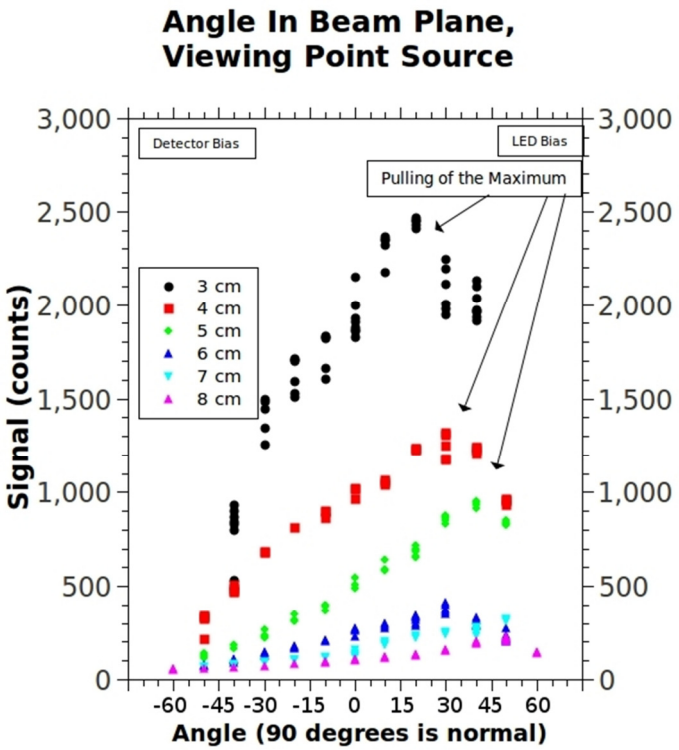

Figure 4
Angle study with angle within beam plane and viewing point source

The second aspect of the angle analysis that was done was to repeat the previous test of the signals vs. angles, but have the fluorometers observing a substrate that would appear to be an infinite plane of fluorescence. The substrate used was previously shown to be similar to algae fluorescence at similar distances when tested with the fluorometers normal to the substrate. The signal curves of the fluorometers were higher than the point tests, and were smoother and more level than the point tests. This leveling can be explained by the averaging effect of allowing the instrument to view fluorescent points closer and further away than the point source experiment.

For the test with the angle perpendicular to the beam plane, the signal showed a decreased decay of the signal at large angles from normal to the substrate, and in comparison the difference was between 10 and 40 percent of the average for the distance. The curves shown in **figure 5** that appeared were more level than the point source, and mostly just showed the

decreasing trend from the physical offset on the instrument. This seems to suggest that when the fluorometer is set up with the angle perpendicular to the beam plane, the signal is fairly constant with respect to the angle from the substrate, so long as the angle is at or within 45 degrees from normal.

Additionally, when the angle is taken within the beam plane, the curve once again is smoother, but retains the maxima seen in the point test. The absolute maximum of the graph seems to be offset more towards 45 degrees from normal, towards the LED beam side. Throughout the distances, the absolute maximum ranges from 30 degrees to 50 degrees for distances of 4 cm and 8 cm respectively. This suggests that if the fluorometer is set up with this orientation the ideal angle will be around 45 degrees when the substrate is between 4 to 8 cm directly out from the face of the instrument. This set of data is shown below in **figure 6** with an account for the dark counts in the signal.

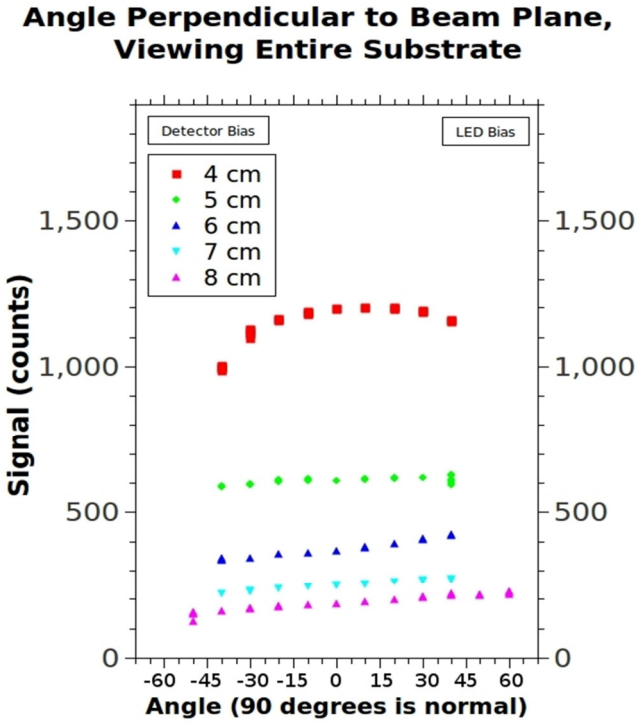

Figure 5
Angle study with angle perpendicular to beam plane and viewing infinite plane

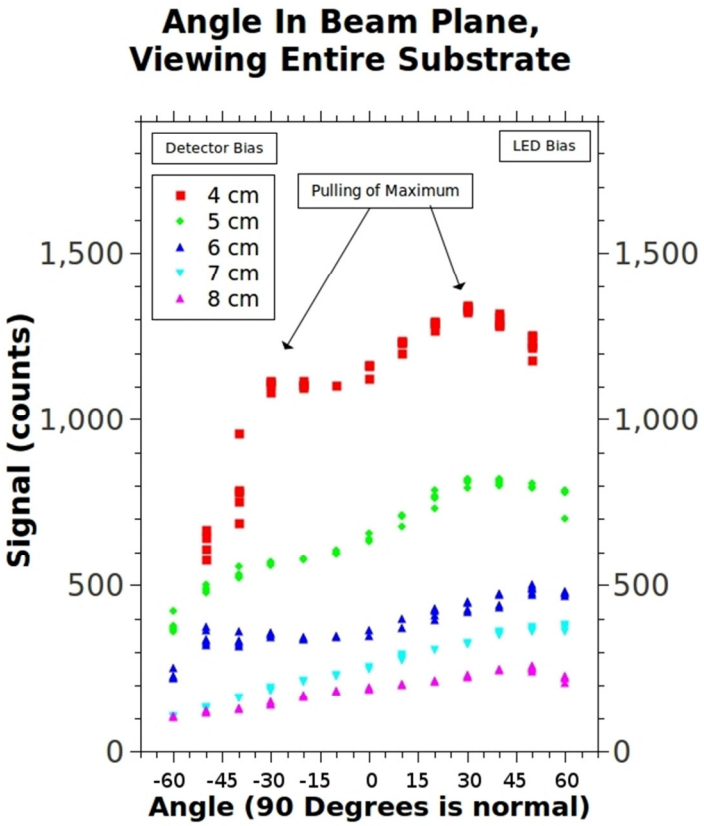

Figure 6
Angle study with angle within beam plane and viewing infinite plane

The results seem to show that for the constrictions of setup on the York River Flume, having the 45 degrees from normal will be possible when the angle is both in the beam plane and perpendicular to it. The difference is that when the angle is in the beam plane, and the angle is towards the LED beam side, the fluorometer will be detecting chlorophyll readings from a more concentrated area of the substrate. When the angle is perpendicular to the beam plane, then it should result in an averaging effect of the substrate, with the area of view being larger than the other setup. Additionally, the data suggests that with the angle perpendicular to the beam plane, if another angle is desired it should be able to perform at a nearly equal level, while when the

angle is within the beam plane the peak performance is limited to between 30 and 50 degrees from normal towards the LED side.

York River Experiments

The first experiment that was done on the York River platform concerning the fluorometer data was to test whether the fluorometer signals would be comparable when they were observing the same substrate. To test this, the fluorometers were deployed from November 4-8 as shown in **figure 7**, with them at 45 degrees to the substrate with the angles perpendicular to the beam plane, so that the signal readings would be affected least by the angle of deployment. Additionally, due to space constrictions on the platform, the fluorometers were deployed observing opposite sides of the same substrate since there was no indication of an algae growth difference between the different sides.

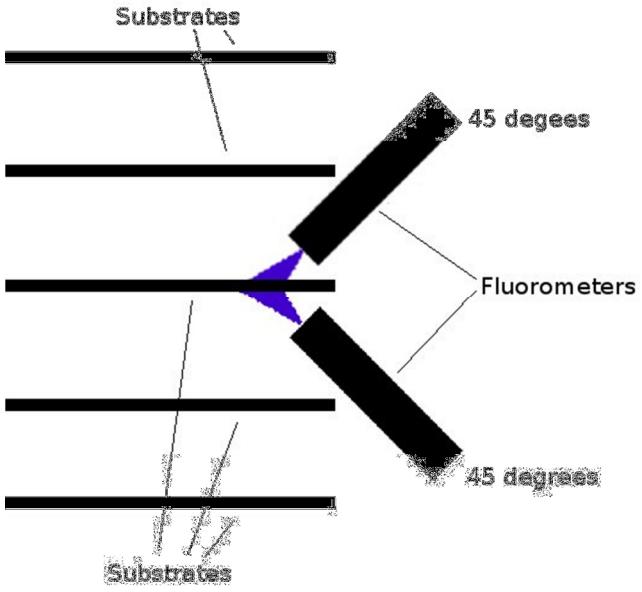

Figure 7
Diagram showing physical setup of fluorometers for comparison and extended deployments

The following data was recorded by both of the fluorometers, and are represented by the averages of each hour with error bars of a single standard deviation. The fluorometers feature a dark count of 50 counts, and in the follows graphs that values is subtracted away to give only the values that are recorded by the fluorometers. This data is too short of a deployment to determine cyclic behavior of the algae, but it does show that despite best efforts being made to deploy the fluorometers in the same orientation and distance from the substrate, the sensitivity of the instruments is too great. The difference between the curves can most likely be attributed to the sensitivity to distance that follows a decaying exponential curve. This shows that the fluorometers can't be mounted so that they give absolute readings on the signal detected from the algae, especially to the level of comparing between two different fluorometers. Although the fluorometers are still useful in this setup to determine the relative change of the signal detected over a deployment. The following graphs show the signal recorded during this deployment, and show the daily average in **figure 8**, the variance per hour in **figure 9**, and factional variance in **figure 10**, with each of these graphs using data without the dark counts of the instruments.

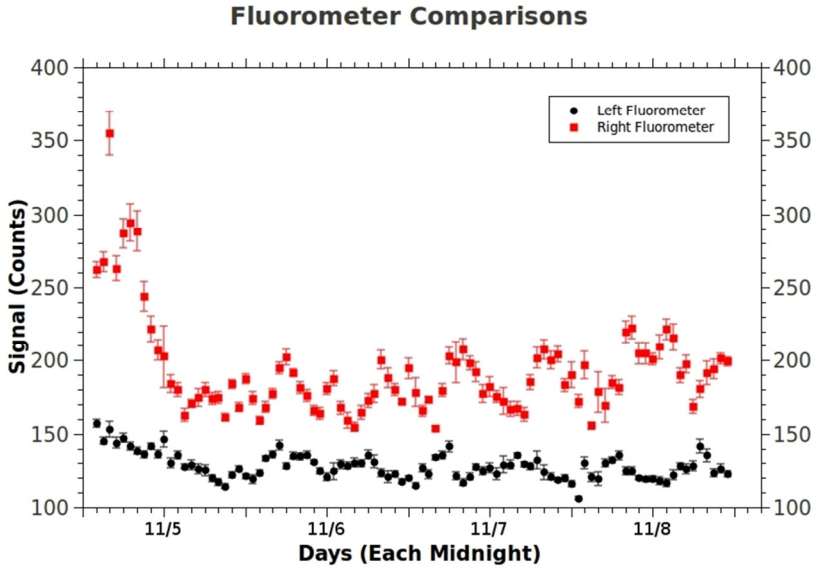

Figure 8
Comparison of recorded hourly averages of fluorometer data from November 4 - 8

In the following **figure 9**, the data of the variance over an hour for each fluorometer is shown. The large variance shown during the first day for the right fluorometer corresponds to an unusually large signal in the comparison, suggesting that the data during that time period was in the presence of an unrecorded variable. The large variance when compared to the size of the signal generated also suggests that the variance seen in this sample is due to the photon collection rather than instrument error, because it varies with the size of the signal. This suggests that the cause of the large initial spike was from a variable such as algae from farther down the flume breaking off and impeding the view of the fluorometer. The floating algae would fluoresce the same as the algae on the substrate and it was floating in the water it would be closer to the instrument and cause this large appearance of growth. Additionally, since the large anomaly is present only for a few hours it suggests that the algae passed through the flume.

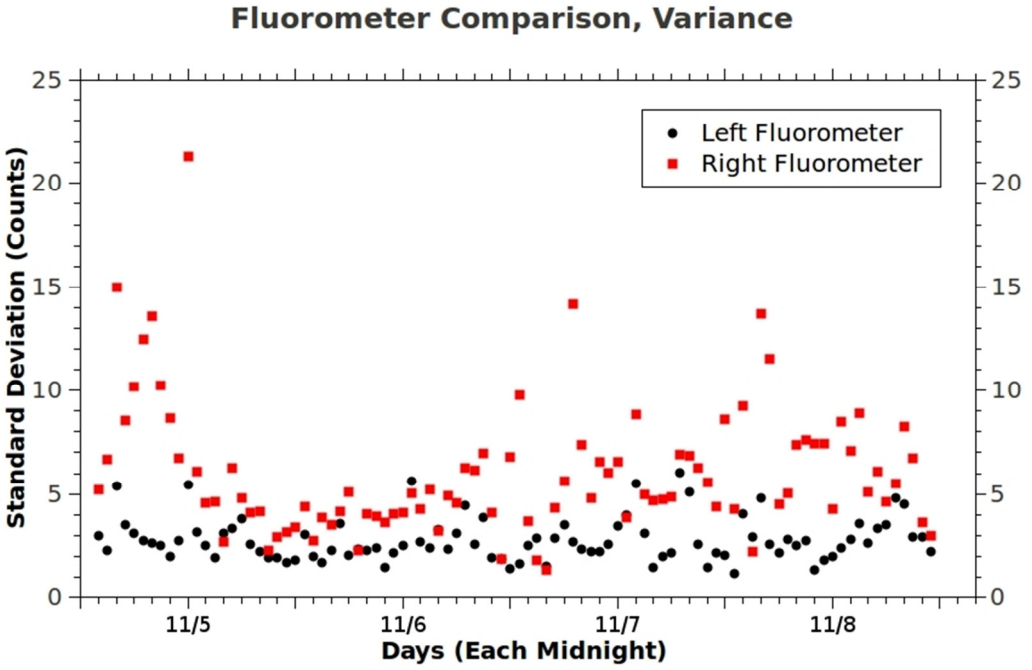

Figure 9
Comparison of recorded hourly average variance of fluorometer data from November 8 - 22

In **figure 10**, the fractional variance of the signal is represented, with it being the standard deviation divided by the average signal for that hour. This shows how the variance is related to the signal with the variance mostly within 5 percent of the signal. This suggests that the using the average of the signals collected each hour is valid, and this is verified by similar results in later deployments.

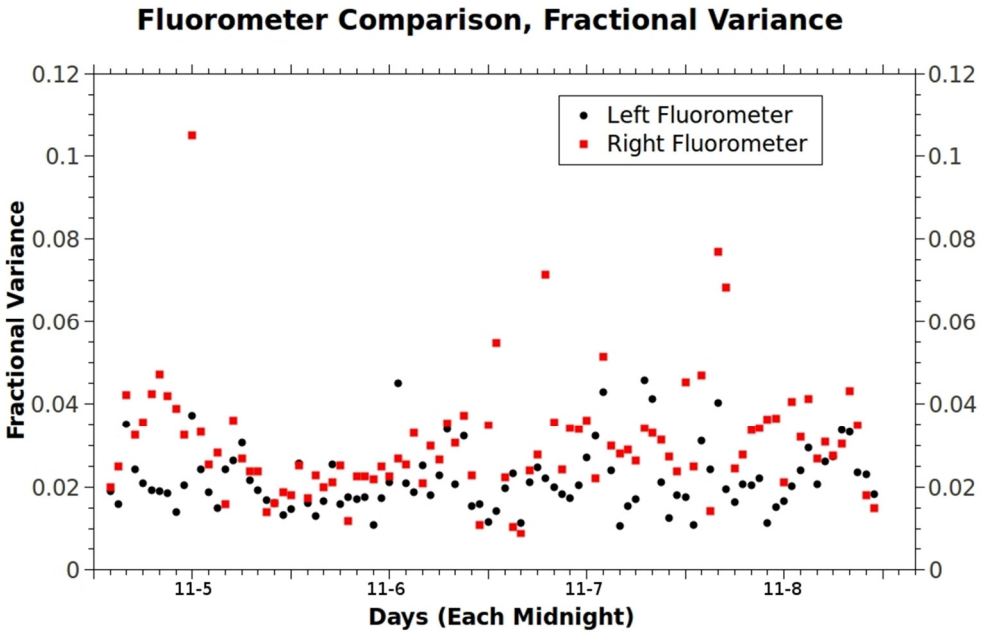

Figure 10
Comparison of recorded hourly average fractional variance of fluorometer data from November 8 - 22

The next experiment was an initial extended deployment of the fluorometer, which was done on November 8 – 22. The deployment retained the setup from the previous comparison experiment, but with only the left fluorometer used due to complications with the right fluorometer. During this deployment, the structure of the signal showed definite signs of cyclical behavior. This structure is shown in the following **figure 11** with the dark counts removed and follows a 24 cycle, with both the maximum and minimum represented between 11 AM and 2 PM. A strong explanation to this can come from photo-inhibition of the chlorophyll. Photo-

inhibition is occurs when chlorophyll is oversaturated by a light source, in this case the sun, and any attempts to further excite the chlorophyll results in a lower than expected reading. This explains why there in a minimum in the signal when compared to readings taken at midnight, when there is no sun. Another sign to confirm this photo-inhibition is a decrease in the variance of the signal, which is discussed in the next section.

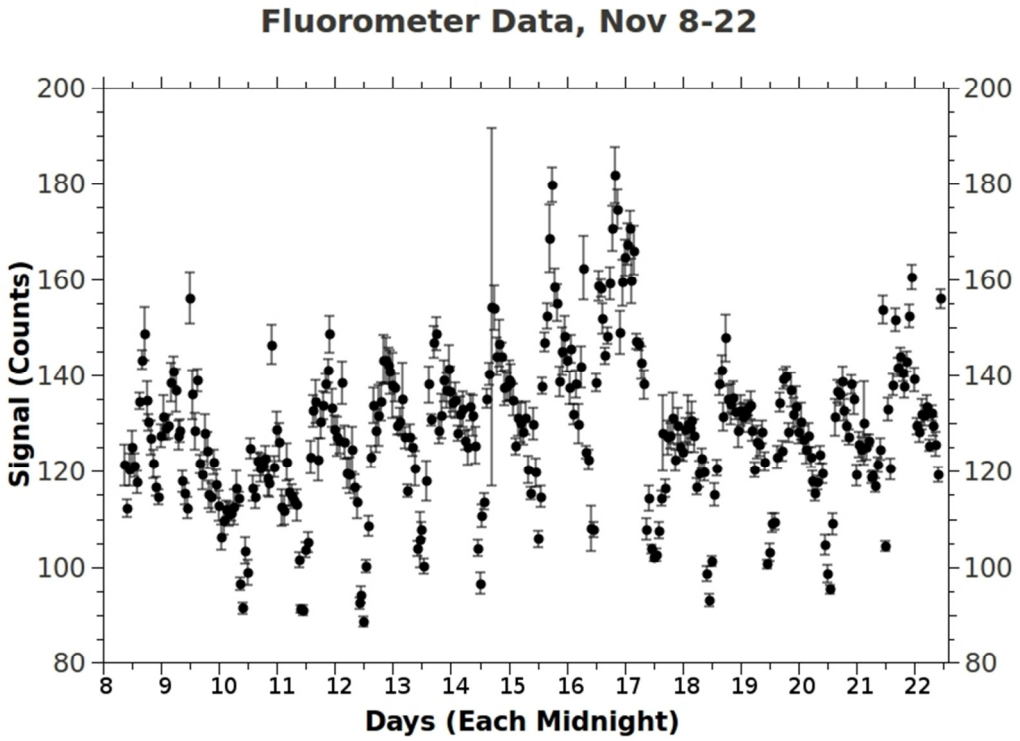

Figure 11
Recorded hourly averages of fluorometer data from November 8 - 22

The following figures show the variance and fractional variance of the data with the dark counts removed. The variance in **figure 12** shows the hourly variance of the data for this deployment, and shows similar structure to the comparison experiment. Initially the variance appears differ greatly throughout each day, but that is due to the large signal differences due to the cyclic nature of the chlorophyll. This is confirmed through **figure 13**, which takes into account the relationship of the variance to the signal it is from, and shows that most of the data has a variance of less than 5 percent of the signal. Additionally, the variance confirms the

previous theory that photo-inhibition occurs due to the low variance during periods of highest sun activity, around noon. This is shown again in **figure 14** with the average variance per hour.

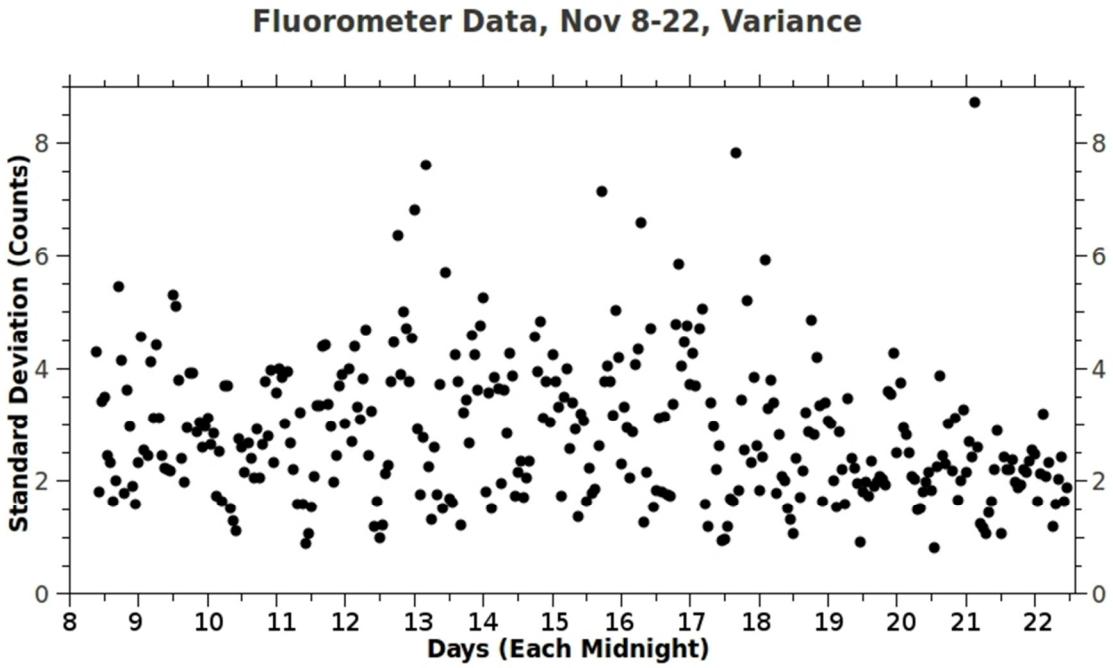

Figure 12
Recorded hourly average variance of fluorometer data from November 8 - 22

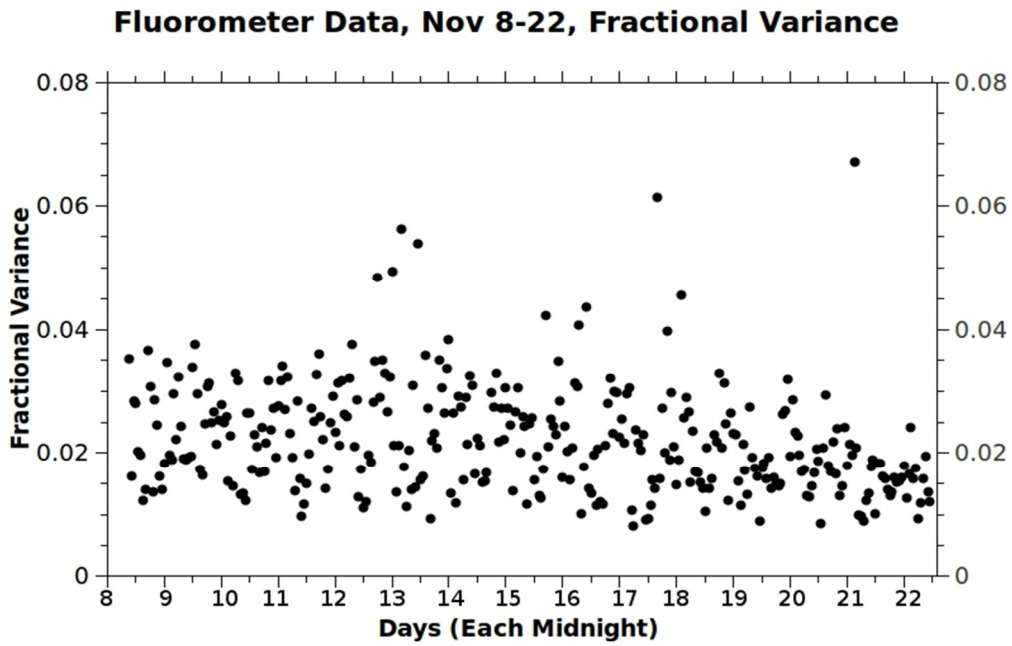

Figure 13
Recorded hourly average fractional variance of fluorometer data from November 8 - 22

In the following graphs the same data is used as above, with the variances averaged for each hour. By looking at the average variance per hour in **figure 14** the trend of lower variance at high solar activity times is more apparent, shows a drop in the variance, while during the rest of the day the average variance is fairly constant. The drop in the variance during this period gives further evidence of photo-inhibition over saturating the chlorophyll, because as the variance decreases it shows that the chlorophyll's ability to fluoresce is inhibited by giving a more constant reading. The fractional variance shown in **figure 15** shows flattening similar to the fluorometer comparison, but the noon drop is still present despite the removal of the factor of variance related to signal strength.

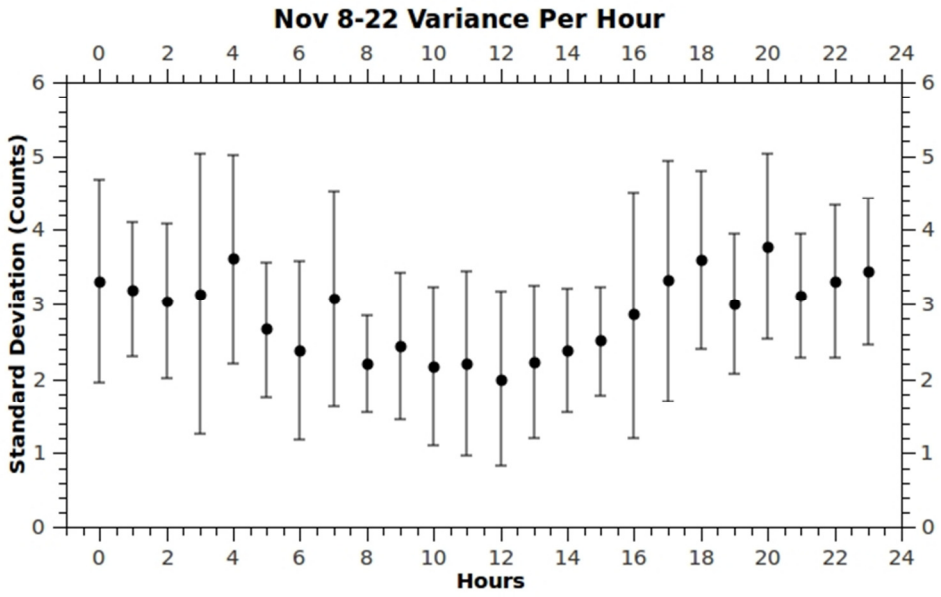

Figure 14
Recorded variance per hour of fluorometer data from November 8 - 22

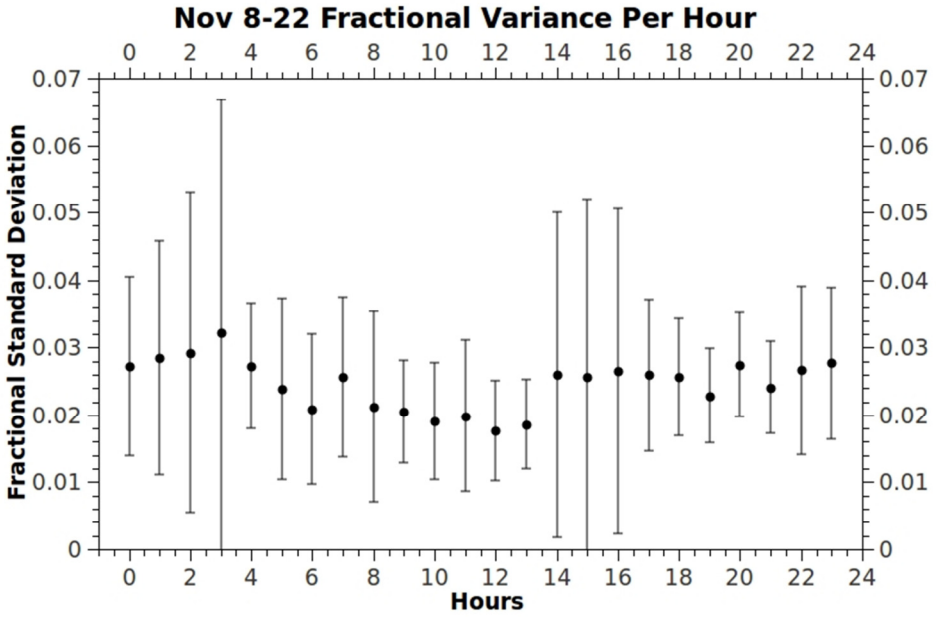

Figure 15
Recorded fractional variance per hour of fluorometer data from November 8 - 22

Another aspect that must be investigated of this deployment is if there is a single value in the original signal data that correlates with the average of the day, which would allow a single value to represent the dataset against the harvest yields. The data shows both a large maximum and minimum between 11AM and 2 PM that is most likely caused by photo-inhibition, and this gives reason to not use these extremes due to the large jump between them. In order to compensate for this, taking the recordings at night would give the most consistent signal readings. In **figure 16** the averages for each day are shown in comparison to the hourly averages and the values that are closest to the averages are the values taken at 2 AM. To show this the daily average is compared to just the 2 AM hour averages in **figure 17**. This relationship between the 2 AM and the daily average is also present in the next deployment done in December. This combined with the variance data showing that photo-inhibition occurs mostly at noon, and thus to remove this factor a time would be needed that was opposite this time, which 2 AM fits into.

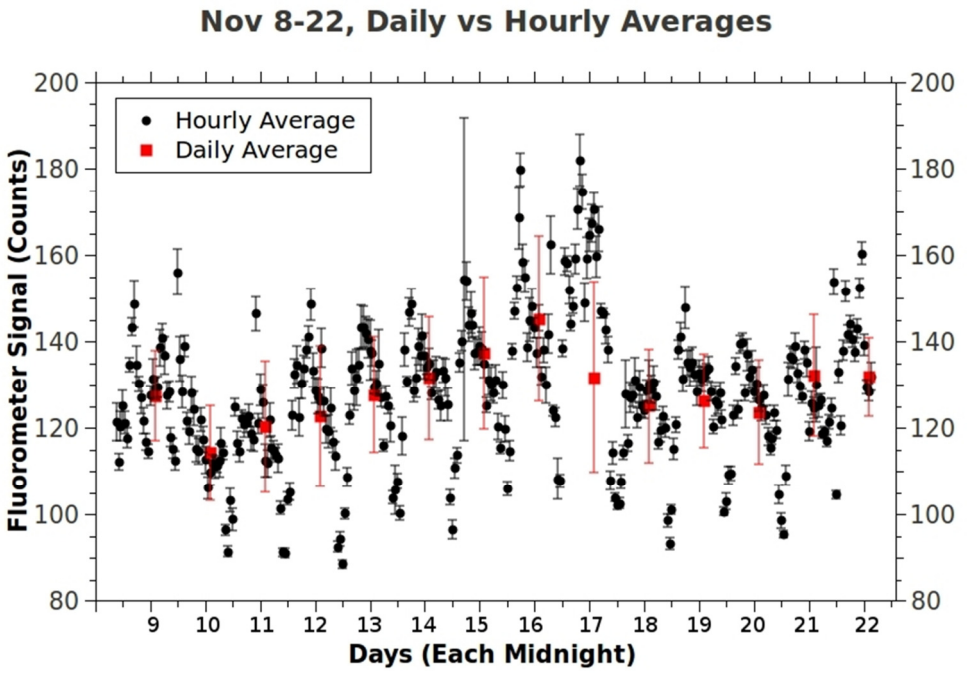

Figure 16
Comparison of recorded hourly vs daily averages of fluorometer data from November 8 - 22

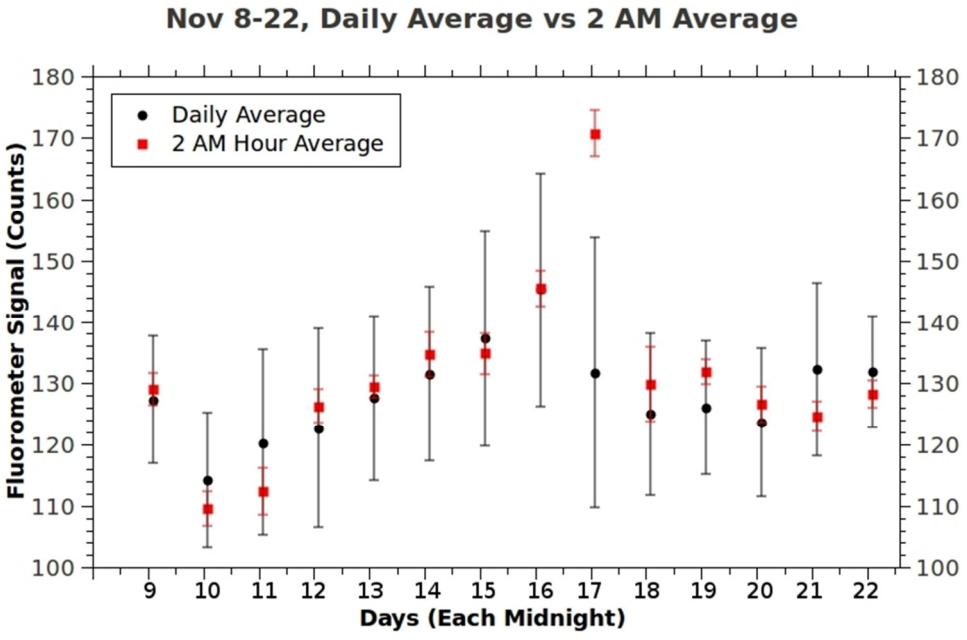

Figure 17
Comparison of recorded 2 AM vs daily averages of fluorometer data from November 8 - 22

This final aspect of the deployment is shown in **figure 18** and features the 2 AM hourly data with dark counts removed and how it relates to harvested data taken from flume. The data on the harvest was taken from an average of all of the screens that were related to the screen that the fluorometer was directed towards. The first two points would be expected to match with the fluorometer signal due to both of them starting with a fresh experiment and harvest. The third point of harvest though is one of continuous growth throughout the entire period, while the screen that the fluorometer was harvested and cleaned when the second point was taken. This data is still useful because the relative growth rates between the days of 18 to 22 and the relative change in the signal during that same period are similar, with the rates being slower than the rest of the deployment. Additionally, after the second harvest when the screen the fluorometer was observing was harvested clean, the fluorometer signal drops accordingly. This drop in the fluorometer signal is a significant display that the fluorometer is in fact observing the fluorescence of the algae rather than the fluorescence of the substrate or the reflection of the original LED beam.

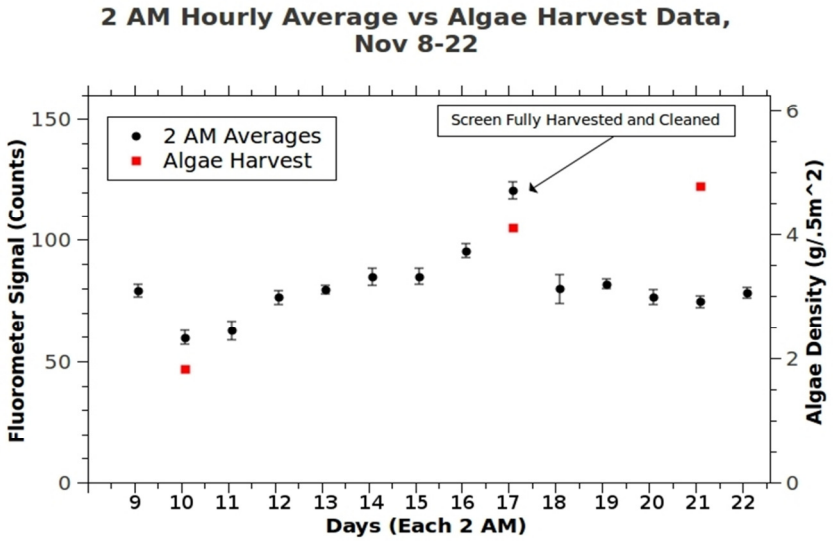

Figure 18
Comparison of recorded 2 AM of fluorometer data against harvest data from November 8 - 22

The next focus of the experiment was to run another extended trial of the fluorometers in the same environment of the York River platform. The deployment was from December 1 – 13 and featured the same setup as the first, with the fluorometer set at 45 degrees to the substrate with the angle perpendicular to the beam plane. In this deployment the following data was recorded, which shows similar structure to the first deployment with noon having the extremes of the hourly data. In the following **figure 19** the hourly averages are again shown with error bars of the standard deviation of the hour and the dark counts removed.

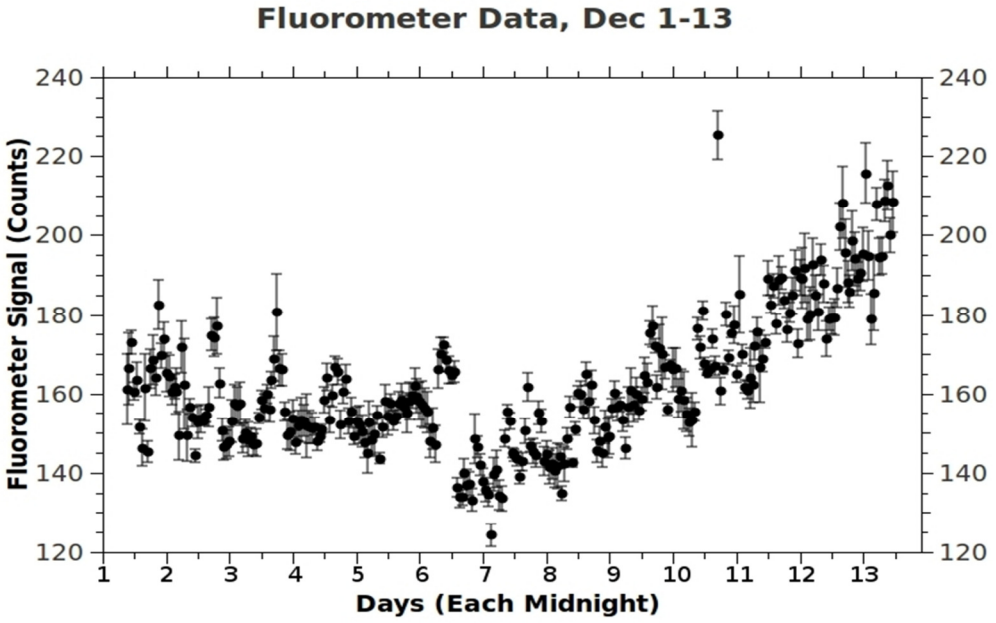

Figure 19
Recorded hourly averages of fluorometer data from December 1 - 13

In the next two graphs the hourly variance and fractional variance is featured from this data without the dark counts. In **figure 20** it shows that the hourly variance decreases during the times of largest solar activity, which suggests again that photo-inhibition is occurring. Due to unknown causes the averages in this deployment have more outliers, though the variance largely does not show anomalies. The lack of anomalies suggests that the outliers are due to the substrate or setup moving, and not due to an instrument error, because the variance is similar to

the other samples and is only increased by the relationship between variance and signal strength. These aspects are also present in the fractional variance along with how a large proportion of the variances are within 4 percent of the signal average.

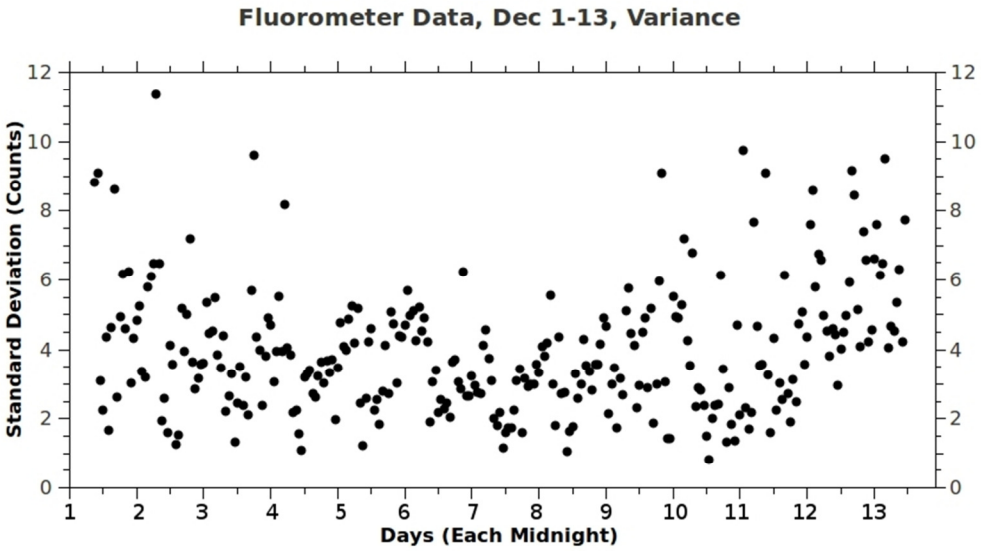

Figure 20
Recorded hourly average variance of fluorometer data for December 1 - 13

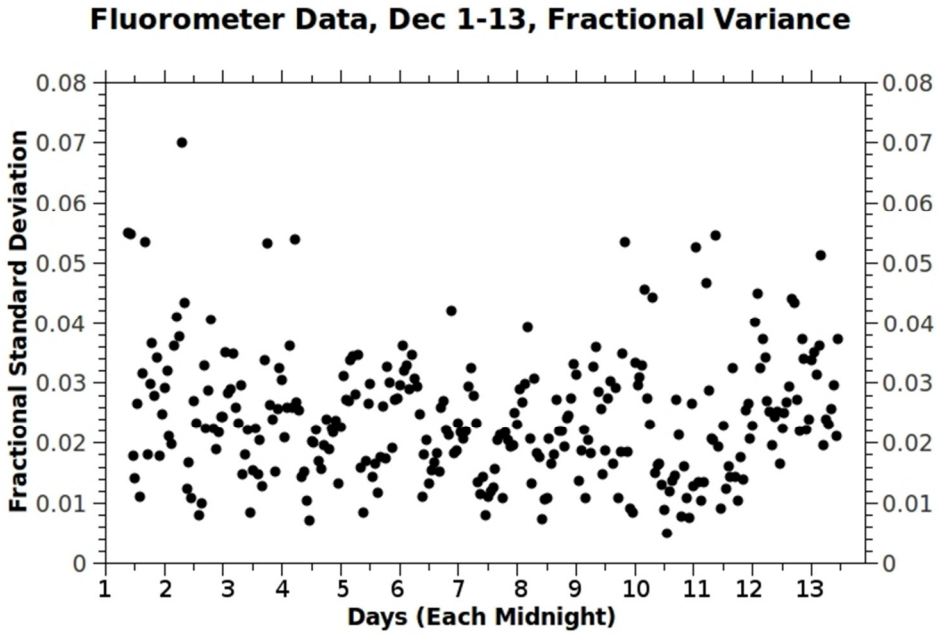

Figure 21
Recorded hourly average fractional variance of fluorometer data from December 1 - 13

Another display of the data confirming the photo-inhibition comes from the following figures of the variance and fractional variance per hour in **figure 22** and **figure 23**. The both of these datasets show at noon the variance decreases where the other hours have fairly constant values. The variance is not as clean as the November deployment, but that can possibly be explained due the flume being towed into the boatyard during the first days of the deployment, and the additional disturbances that the flume would experience due to the closer proximity to the shore and other working vessels. An interesting aspect is how despite this, the signals recorded and the variances of the data don't differ greatly from the previous undisturbed deployment. This suggests that so long as the substrate and fluorometer are in a fixed position to each other, the other factors occurring on the flume may be less important than previously believed.

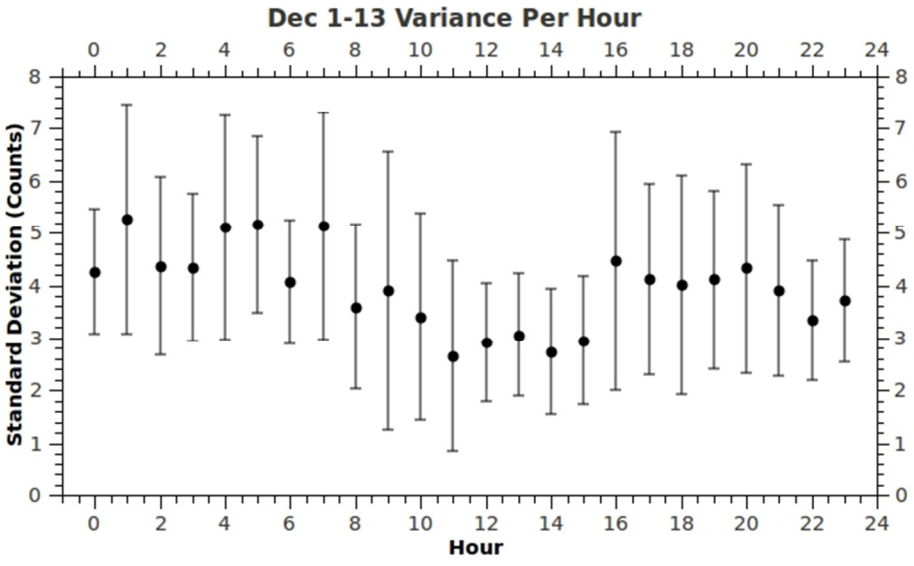

Figure 22
Recorded variance per hour of fluorometer data from December 1 - 13

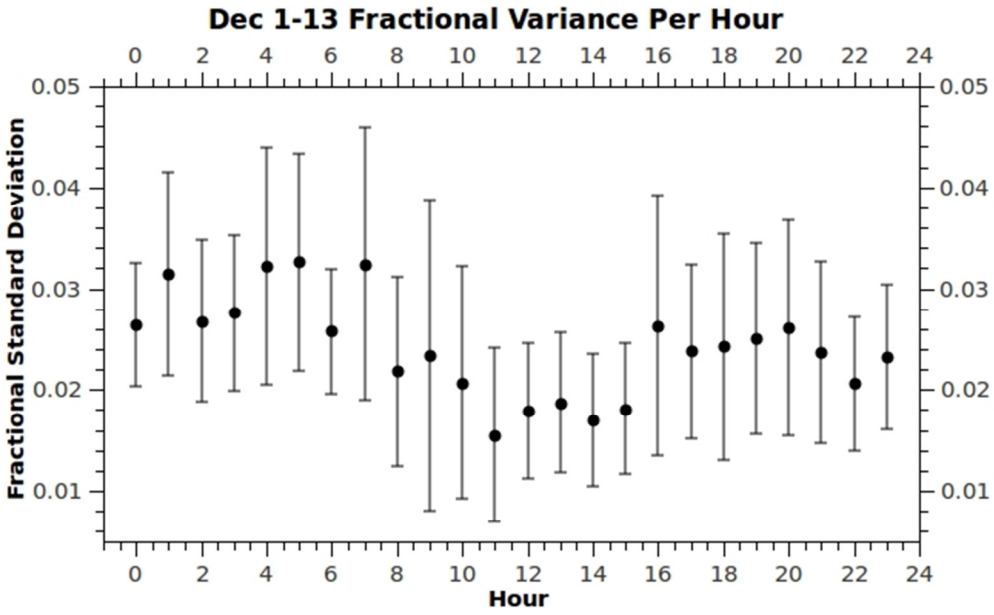

Figure 23
Recorded fractional variance per hour of fluorometer data from December 1 - 13

Next, there was to find a time of the day that would be able to represent in the future, what the average of the day would be closest to. When the daily average was placed on the same plot as all of the hourly averages in **figure 24** and **figure 25** with the dark counts removed, the 2 AM value as previously found was again a best fit. Again both the maximum and minimum are present in the data within an hour of each other and thus it seems best to use the time of 2 AM to represent the most consistent value to represent the day. The 2 AM time period doesn't fit the daily average quite as well as in the previous deployment, but the uncertainties of both of the values remain within each other. The time that the two averages differ the most is directly after the full harvest on the 6th, but the difference is resolved after that.

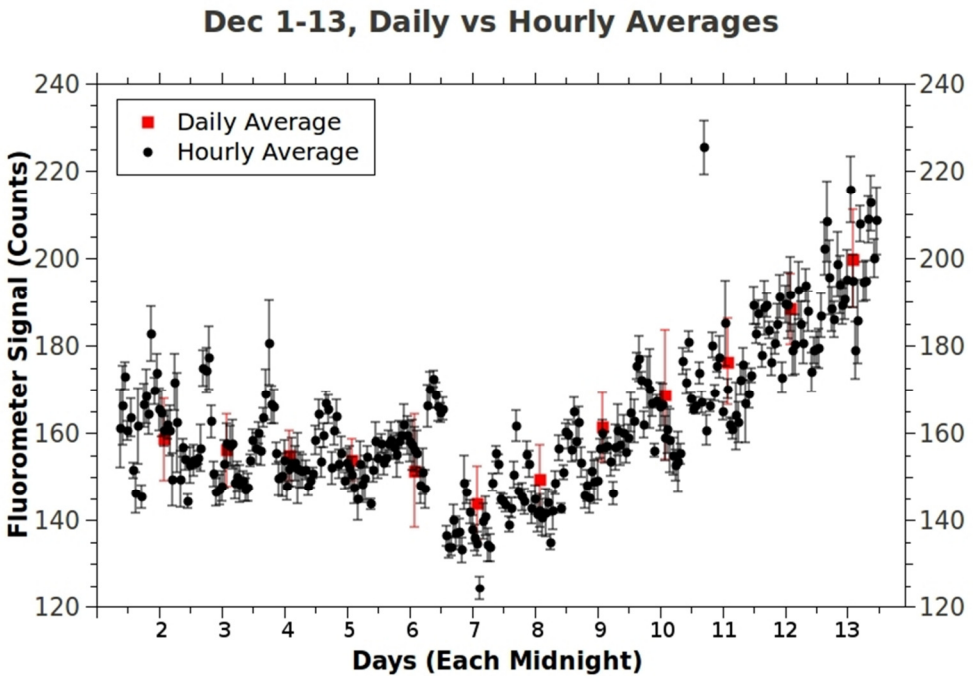

Figure 24
Comparison of recorded hourly vs daily averages of fluorometer data from December 1 - 13

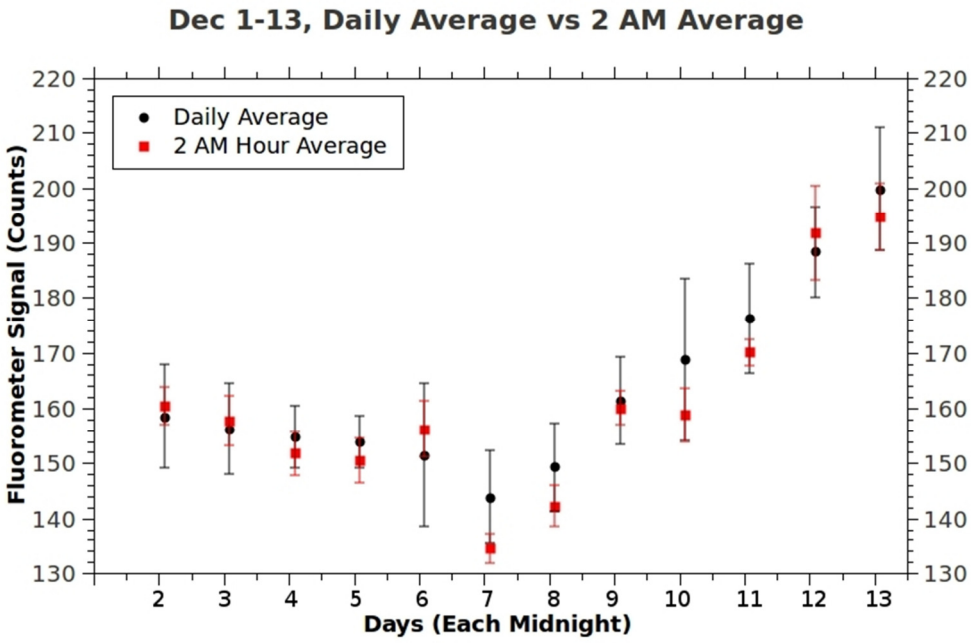

Figure 25
Comparison of recorded 2 AM vs daily averages of fluorometer data from December 1 - 13

The final aspect of this deployment was to again compare the 2 AM hourly average found to be able to represent a cleaner form of the deployment data to the harvest data taken of each substrate that represented the screen the fluorometer was directed towards. In **figure 26** the comparison between the 2 AM without dark counts and harvest data is shown. Unfortunately the harvest data available during this time period was of growth that was undisturbed growth for longer than the substrate that the fluorometer was directed towards was able to grow. The relative growth is still comparable, but not as relevant as during the November deployment for direct comparison of growth rates. Also this deployment featured a point of December 6th when the screen the fluorometer was directed towards was scraped clean to take the substrate back to an initial state. This shows how the signal decreases immediately during that time similar to the previous deployment, confirming how the fluorometer was observing fluorescence of algae. Another interesting aspect of this is if the assumption that the fluorometer was observing the algal growth, then the growth increased rapidly after the clean harvest, suggesting that the harvest stimulated more growth of algae that fluoresced than there was previously on the substrate.

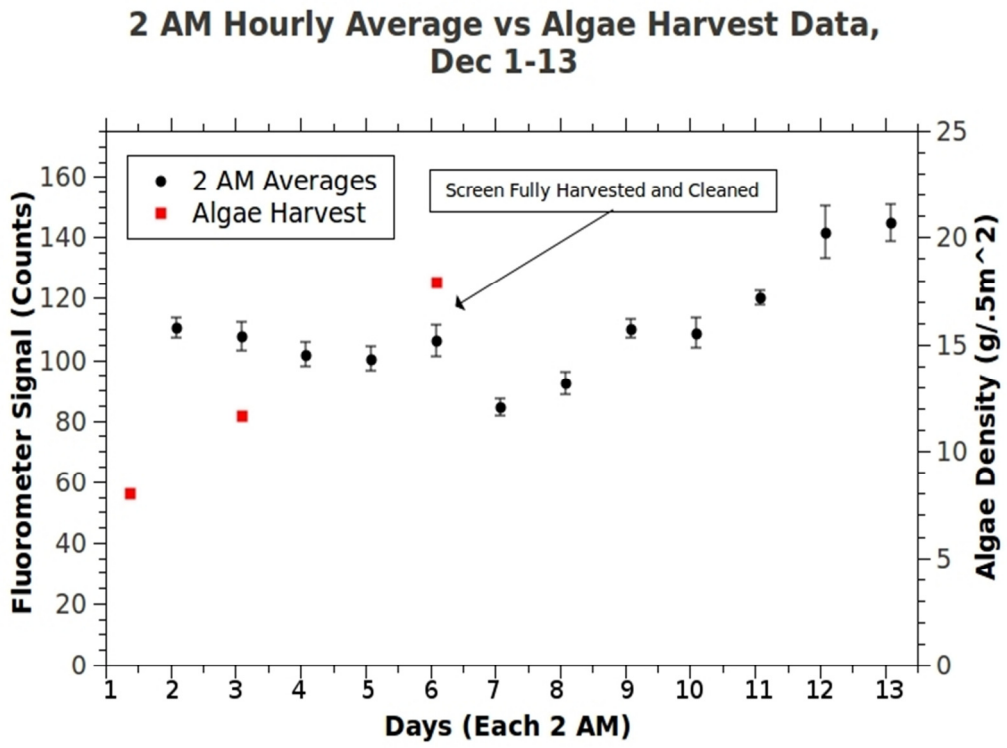

Figure 26
Comparison of recorded 2 AM of fluorometer data against harvest data from December 1 - 13

Conclusions

During this project I was posed with the objective to characterize the WetLabs FLNTUSB fluorometer and to determine if it was possible to measure the fluorescence to plot the growth of wild algae. I determined that there are two setups possible when deploying the fluorometer, either having the angle of deployment in or perpendicular to the beam plane created by the LED and Detector absorption cones. If the angle is within the beam plane then the largest maximum and most stable angle will be around 45 degrees towards the LED beam side. If the angle is perpendicular to the beam plane the angle sensitivity is decreased from the previous setup, and the angle is able to handle whatever angle the physical constraints are, though an angle of more than 45 degrees is not recommended.

The next aspect was to deploy the fluorometers for extended periods, and through doing so I determined that the fluorometers are useful to measure relative changes in signal, that can be correlated to fluorescence of the algae. They are not able to be compared directly to each other due to the high sensitivity to the instruments based on distance and angle, though once installed in a fixed position the sensitivity of the fluorometer seems to vary greatly when other variables are changed in the experiment. The fluorescence of the chlorophyll is dependent on the photo-inhibition effect, though if the daily measurements are taken around 2 AM the values recorded are very close to representing the daily average without experiencing the period photo-inhibition. Finally, there is evidence that the fluorescence observed by the fluorometers can be correlated to the algae density of the substrate that it is directed towards.

Data Tables, Lab Experiment - Angle Sensitivity

In Beam Plane With Point Source											
3 cm			4 cm			5 cm			6 cm			7 cm	
Angle	Signal (Counts)		Angle	Signal (Counts)		Angle	Signal (Counts)		Angle	Signal (Counts)		Angle	Signal (Counts)
130	2128		140	934		140	838		140	222		140	310
130	2099		140	962		140	831		140	205		140	314
130	1915		140	965		140	825		140	209		140	318
130	2035		140	959		140	835		140	213		140	320
130	1970		140	954		140	839		140	232		140	321
130	1935		140	965		140	851		140	273		140	315
130	1975		140	965		130	912		130	284		130	259
130	1963		130	1206		130	930		130	289		130	234
130	1965		130	1222		130	943		130	319		130	251
120	1982		130	1221		130	950		130	332		130	275
120	2002		130	1235		130	945		130	331		130	277
120	2113		130	1243		130	951		130	329		130	278
120	2244		120	1176		120	861		120	402		120	250
120	2192		120	1177		120	828		120	412		120	245
120	2114		120	1250		120	848		120	413		120	246
120	1945		120	1305		120	860		120	347		120	243
110	2427		120	1317		120	868		120	372		120	252
110	2470		110	1221		120	876		120	362		120	251
110	2455		110	1229		110	718		110	288		110	236
110	2451		110	1237		110	657		110	320		110	222
110	2457		110	1232		110	655		110	340		110	220
110	2456		110	1238		110	687		110	333		110	220
110	2410		100	1041		110	692		110	332		110	220
100	2353		100	1052		110	696		110	300		110	219
100	2348		100	1054		100	643		100	275		100	205
100	2355		100	1052		100	589		100	287		100	189
100	2367		100	1067		100	587		100	298		100	185
100	2366		90	967		100	584		100	299		100	187
100	2320		90	962		100	586		100	298		100	186
100	2177		90	1016		100	583		100	284		100	185
90	2149		90	1019		90	547		90	274		90	160
90	1999		90	1016		90	506		90	269		90	139
90	1928		80	865		90	490		90	266		90	128
90	1910		80	895		90	488		90	262		90	124
90	1879		80	899		90	489		90	262		90	123

90	1867		80	898		90	490		90	230		90	127
90	1857		80	902		80	400		80	205		80	123
90	1829		70	815		80	370		80	208		80	112
80	1602		70	815		80	396		80	207		80	112
80	1663		70	815		80	397		80	208		80	113
80	1832		70	813		80	396		80	209		80	115
80	1833		70	812		80	397		80	202		80	120
80	1829		60	688		70	352		70	178		70	110
80	1821		60	681		70	311		70	177		70	100
70	1594		60	681		70	312		70	175		70	107
70	1511		60	679		70	315		70	174		70	107
70	1705		60	676		70	314		70	173		70	107
70	1706		50	507		70	313		70	162		70	107
70	1697		50	490		60	265		60	145		60	92
70	1713		50	488		60	235		60	144		60	88
70	1530		50	477		60	234		60	143		60	89
60	1347		50	468		60	231		60	141		60	90
60	1484		40	325		60	227		60	140		60	89
60	1495		40	332		60	225		60	124		60	89
60	1483		40	341		50	187		50	108		50	83
60	1447		40	340		50	164		50	108		50	77
60	1255		40	337		50	165		50	106		50	77
50	530		40	213		50	166		50	105		50	77
50	796					50	165		50	103		50	76
50	899					50	166		50	87		50	75
50	832					40	142		40	70		40	65
50	845					40	115		40	75		40	69
50	870					40	124		40	76		40	69
50	931					40	129		40	75		40	69
						40	129		40	75		40	68
						40	130		40	72		40	69

Perpendicular to Beam Plane With Point Source											
3 cm			4 cm			5 cm			6 cm			7 cm	
Angle	Signal (Counts)		Angle	Signal (Counts)		Angle	Signal (Counts)		Angle	Signal (Counts)		Angle	Signal (Counts)
120	2225		130	913		130	486		140	182		140	112
120	2231		130	933		130	489		140	180		140	111
120	2242		130	935		130	488		140	183		140	111
120	2245		130	952		130	477		140	185		140	113
120	2252		130	963		130	476		140	187		140	126
120	2265		130	1060		130	483		140	218		140	129
110	2320		120	1119		120	487		130	264		130	146
110	2334		120	1120		120	485		130	256		130	145
110	2337		120	1125		120	485		130	246		130	145
110	2339		120	1143		120	483		130	249		130	145
110	2352		120	1152		120	484		130	250		130	145
110	2364		120	1168		120	481		130	254		130	146
100	2392		110	1178		110	482		120	281		120	157
100	2394		110	1182		110	479		120	286		120	158
100	2390		110	1174		110	476		120	288		120	157
100	2387		110	1174		110	477		120	288		120	157
100	2389		110	1177		110	470		120	288		120	158
100	2399		110	1166		110	473		120	290		120	159
90	2406		100	1145		100	475		110	295		110	161
90	2407		100	1144		100	469		110	295		110	162
90	2407		100	1138		100	467		110	294		110	162
90	2407		100	1135		100	467		110	292		110	160
90	2408		100	1136		100	467		110	285		110	160
90	2388		100	1127		100	467		110	282		110	160
80	2321		90	1081		90	443		100	233		100	157
80	2317		90	1052		90	440		100	221		100	156
80	2321		90	1102		90	441		100	245		100	154
80	2319		90	1173		90	441		100	243		100	153
80	2320		90	1173		90	442		100	245		100	153
80	2300		90	1162		90	441		100	245		100	155
70	2187		80	1010		80	393		90	253		90	159
70	2206		80	1007		80	395		90	256		90	158
70	2214		80	1037		80	395		90	261		90	157
70	2225		80	1070		80	397		90	261		90	157
70	2224		80	1075		80	398		90	260		90	158
70	2195		80	1076		80	396		90	258		90	156
60	2065		70	1033		70	348		80	239		80	151

60	2093		70	1022		70	354		80	235		80	150
60	2086		70	1021		70	362		80	234		80	150
60	2066		70	1031		70	362		80	230		80	149
60	2040		70	1035		70	362		80	227		80	149
60	1859		70	1025		70	357		80	227		80	148
50	1648		60	903		60	259		70	210		70	135
50	1676		60	917		60	283		70	205		70	134
50	1733		60	946		60	285		70	204		70	134
50	1805		60	950		60	282		70	203		70	134
50	1732		60	922		60	281		70	202		70	135
			60	907		60	257		70	200		70	133
			50	723		50	202		60	180		60	125
			50	719		50	198		60	183		60	126
			50	729		50	210		60	185		60	124
			50	753		50	214		60	186		60	125
			50	754		50	216		60	186		60	123
			50	748		50	219		60	186		60	122
									50	166		50	111
									50	163		50	110
									50	164		50	110
									50	165		50	109
									50	166		50	109
									50	164		50	108
									40	140		40	91
									40	137		40	89
									40	137		40	89
									40	137		40	89
									40	138		40	89
									40	138		40	89

In Beam Plane With Infinite Plane Source											
3 cm			4 cm			5 cm			6 cm			7 cm	
Angle	Signal (Counts)		Angle	Signal (Counts)		Angle	Signal (Counts)		Angle	Signal (Counts)		Angle	Signal (Counts)
130	2317		140	1254		150	701		150	474		150	370
130	2318		140	1249		150	779		150	480		150	381
130	2302		140	1177		150	786		150	480		150	380
130	2292		140	1215		150	780		150	478		150	382
130	2286		140	1221		150	783		150	466		150	379
130	2292		140	1229		150	780		150	481		150	361
120	2383		130	1279		140	795		140	488		140	361
120	2454		130	1290		140	796		140	492		140	368
120	2458		130	1285		140	798		140	494		140	376
120	2458		130	1309		140	807		140	500		140	361
120	2467		130	1317		140	792		140	477		140	365
120	2462		130	1319		140	794		140	469		140	362
110	2469		120	1321		130	800		130	471		130	350
110	2491		120	1338		130	814		130	469		130	351
110	2492		120	1333		130	822		130	470		130	353
110	2501		120	1322		130	818		130	472		130	359
110	2500		120	1343		130	822		130	434		130	362
110	2510		120	1327		130	807		130	438		130	356
100	2498		110	1287		120	817		120	445		120	322
100	2495		110	1286		120	813		120	446		120	325
100	2499		110	1293		120	811		120	445		120	327
100	2502		110	1291		120	816		120	448		120	327
100	2502		110	1286		120	820		120	424		120	328
100	2502		110	1268		120	793		120	419		120	328
90	2488		100	1232		110	786		110	423		110	305
90	2472		100	1235		110	771		110	426		110	305
90	2464		100	1235		110	762		110	427		110	305
90	2465		100	1230		110	765		110	428		110	306
90	2464		100	1230		110	766		110	408		110	306
90	2461		100	1199		110	731		110	396		110	307
80	2432		90	1163		100	709		100	397		100	292
80	2380		90	1164		100	711		100	397		100	287
80	2377		90	1163		100	712		100	397		100	280
80	2377		90	1162		100	713		100	397		100	283
80	2377		90	1160		100	713		100	398		100	283
80	2377		90	1122		100	679		100	372		100	276
70	2410		80	1104		90	657		90	363		90	256

70	2428		80	1104		90	639		90	365		90	255
70	2421		80	1103		90	633		90	364		90	254
70	2418		80	1103		90	639		90	364		90	255
70	2417		80	1102		90	639		90	363		90	255
70	2417		70	1102		90	639		90	348		90	250
70	2507		70	1106		80	607		80	343		80	227
60	2542		70	1116		80	596		80	344		80	228
60	2434		70	1095		80	596		80	345		80	230
60	2429		70	1097		80	594		80	346		80	231
60	2439		70	1097		80	595		80	345		80	230
60	2446		60	1106		80	599		80	346		80	229
60	2554		60	1115		70	577		70	340		70	214
50	2615		60	1117		70	577		70	338		70	213
50	2594		60	1115		70	577		70	338		70	213
50	2589		60	1116		70	578		70	339		70	212
50	2587		60	1084		70	580		70	340		70	212
50	2583		50	957		70	578		70	344		70	210
			50	785		60	570		60	345		60	194
			50	751		60	568		60	352		60	187
			50	688		60	560		60	355		60	186
			50	754		60	560		60	356		60	184
			50	780		60	561		60	355		60	184
			40	669		60	562		60	353		60	183
			40	577		50	554		50	335		50	160
			40	610		50	530		50	331		50	163
			40	644		50	532		50	316		50	162
			40	642		50	522		50	318		50	162
			40	642		50	521		50	322		50	162
						50	524		50	361		50	160
						40	499		40	376		40	125
						40	491		40	365		40	129
						40	478		40	319		40	132
						40	477		40	332		40	132
						40	478		40	338		40	133
						40	482		40	326		40	133
						30	421		30	251		30	101
						30	377		30	229		30	102
						30	370		30	225		30	102
						30	367		30	225		30	103
						30	361		30	224		30	104

Perpendicular to Beam Plane With Infinite Plane Source									
3 cm		4 cm		5 cm		6 cm		7 cm	
Angle	Signal (Counts)	Angle	Signal (Counts)	Angle	Signal (Counts)	Angle	Signal (Counts)	Angle	Signal (Counts)
120	2105	130	1155	130	627	130	425	130	268
120	2104	130	1153	130	624	130	423	130	269
120	2107	130	1160	130	595	130	420	130	270
120	2106	130	1155	130	602	130	422	130	271
120	2109	130	1153	130	609	130	422	130	271
120	2111	130	1153	130	611	130	423	130	272
110	2125	120	1183	120	617	120	408	130	273
110	2134	120	1189	120	618	120	410	130	273
110	2142	120	1187	120	618	120	409	120	268
110	2147	120	1189	120	617	120	409	120	268
110	2148	120	1187	120	618	120	409	120	268
110	2152	120	1187	120	618	120	407	120	267
100	2182	110	1197	110	617	110	393	120	268
100	2189	110	1198	110	616	110	392	120	268
100	2194	110	1199	110	617	110	393	120	268
100	2195	110	1194	110	618	110	393	120	266
100	2198	110	1194	110	618	110	393	110	261
100	2201	110	1200	110	617	110	392	110	261
90	2244	100	1198	100	613	100	380	110	261
90	2254	100	1200	100	610	100	380	110	261
90	2259	100	1200	100	612	100	380	110	261
90	2260	100	1199	100	612	100	378	110	261
90	2261	100	1199	100	613	100	378	110	261
90	2260	100	1200	100	612	100	377	110	260
80	2255	90	1196	90	607	90	366	100	254
80	2260	90	1196	90	607	90	367	100	253
80	2258	90	1195	90	607	90	367	100	253
80	2261	90	1194	90	607	90	368	100	252
80	2262	90	1194	90	607	90	368	100	253
80	2262	90	1193	90	607	90	368	100	253
70	2305	80	1186	80	613	80	360	100	253
70	2332	80	1185	80	611	80	359	100	252
70	2331	80	1182	80	608	80	359	90	249
70	2329	80	1179	80	608	80	360	90	249
70	2329	80	1178	80	608	80	360	90	249
70	2329	80	1175	80	609	80	360	90	249
60	2351	70	1161	70	611	70	357	90	249

60	2355		70	1160		70	607		70	357		90	249
60	2357		70	1160		70	604		70	357		90	249
60	2356		70	1158		70	604		70	356		90	248
60	2350		70	1156		70	603		70	355		80	244
60	2356		70	1154		70	604		70	355		80	243
50	2368		60	1123		60	596		60	343		80	244
50	2350		60	1126		60	596		60	343		80	244
50	2320		60	1123		60	592		60	343		80	243
50	2320		60	1115		60	593		60	344		80	243
50	2316		60	1109		60	594		60	344		80	243
50	2299		60	1096		60	593		60	344		80	243
			50	1004		50	587		50	342		70	238
			50	999		50	591		50	341		70	238
			50	996		50	590		50	339		70	238
			50	994		50	589		50	338		70	238
			50	996		50	590		50	338		70	238
			50	984		50	589		50	336		70	238
												70	238
												70	236
												60	227
												60	227
												60	228
												60	228
												60	227
												60	227
												60	227
												60	225
												50	218
												50	219
												50	219
												50	219
												50	219
												50	220
												50	219
												50	219

Bibliography

Aberle, N. (September 2006). 'Spectral fingerprinting' for specific algal groups on sediments in situ: a new senso. *Stuttgart* , 575-592.

H, U. (1958). Zur Vervollkommnung der quantitativen Phytoplankton-Methodik. *Mitt. Internat.* , 1-38.

SCCF Recon. (2010). *Chlorophyll.* Retrieved August 1, 2010, from SCCF Recon - Sanibel-Captiva Conservation Foundation: River, Estuary and Coastal Observing Network: http://recon.sccf.org/definitions/chlorophyll.shtml

Schroeder, W. &. (1994). Pigment patterns in suspended matter from Elbe and associated waters as determined using high performance liquid chromatography. *Neth. J Aquat. Ecol.* , 255-265.

Wetlabs. (May 17, 2010). *Characterization Sheet.*

Wetlabs. (23 Dec 2009). *Combination Fluorometer and Turbidity Sensor.*